3. EARTHQUAKE GROUND MOTION

3.1 Overview

At 1:47 am (local time) on September 21, 1999, an earthquake with magnitude 7.3 occurred 150 km southwest of Taipei. As of October 6, 1999 the casualties, number of injured and missing persons were 2295, 8731 and 92.

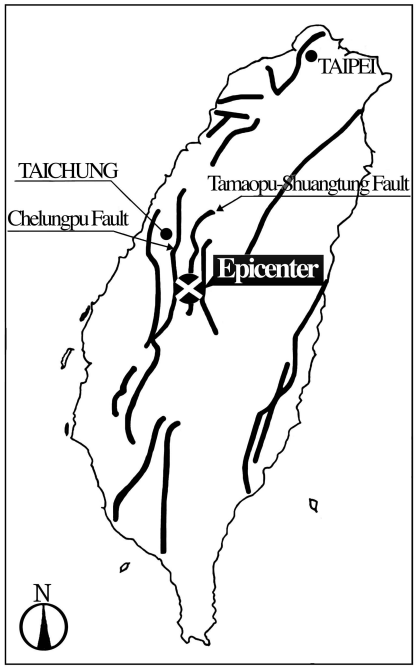

Figure 3.1 Epicenter and Faults

The number of collapsed houses was 9 thousand and several hundreds. Because the epicenter was located near Ji-Ji in Nan-Tou prefecture in Taiwan this earthquake named the 1999 Ji-Ji earthquake. This earthquake reportedly caused by the movement of the Chelongpu fault (from Da-Jia Shi river to Juo-Shoei Shi river). This is a thrust type fault with dip angle about 30 degree. The west side of the Chelongpu fault was the foot wall and rose up 1-4 m to the west side. The damage in the region from Dong-Shyh to Chao-Tuen located on the hanging wall was severe. The length and width of this earthquake fault are 80 km and 40 km. The maximum dislocation measured at ground surface was 6.5 m.

More than 700 strong motion observation stations are distributed and maintained by the Central Weather Bureau, Ministry of Transportation and Communications, Taiwan. About 70 percent of observation station was triggered. Based on recorded earthquake motions the detail study on the rupture process of the earthquake fault will be done because spatial distribution of predominant periods and durations of strong motions along the Chelongpu fault shows a possibility to exist lather big asperity compared to the 1995 Hyogoken Nambu earthquake. The average distance of observation stations near the Chelongpu fault is several kilometers. Observed records at these stations will be used extensively to investigate mechanisms of damage to structures.

3.2 Seismic Environment and Historical Earthquake

Figure 3.2 and Table 3.1 show large historical events in Taiwan from 1904 to 1986. The damage caused by the 1904 earthquake was surveyed by the special Japanese reconnaissance team which leaded by Dr. Makino as a chairman and Dr. Ohmori as a secretary. During this earthquake the Tachienshan and the Chukou faults were moved which is located at south of Chelungpu fault. Figure 3.3 shows the number of earthquakes occurred in 1904. Figure 3.4 is the strongly affected area where the main earthquake energy was released. Both of areas coincide well.

In Taiwan three large historical events were occurred in 1935 (*M*7.1), 1941 (*M*7.1), and 1964 (*M*7.0) (Bonilla, 1977). The destructive earthquakes have occurred along the western foothills from Chutung to Tainan (see Figure3.5).

Table 3.1 Historic Earthquakes in Taiwan

表 0001・台灣十大災害地震和地震系列震源參數一覽表

編號	地震名稱	發震時間 (120°E)	震央位置		震源深度 (公里)	地震規模 (M_L)
			北緯(N)	東經(E)		
1	斗六地震	1904/11/06 04:25	23.575	120.250	7.0	6.1
2	梅山地震	1906/03/17 06:43	23.550	120.450	6.0	7.1
3	南投地震系列	1916/08/28 15:27	24.000	121.025	45.0	6.8
		1916/11/15 06:31	24.100	120.875	3.0	6.2
		1917/01/05 00:55	24.000	120.975	很淺	6.2
		1917/01/07 02:08	23.950	120.975	很淺	5.5
4	新竹—台中地震	1935/04/21 06:02	24.350	120.817	5.0	7.1
5	中埔地震	1941/12/17 03:19	23.400	120.475	12.0	7.1
6	新化地震	1946/12/05 06:47	23.070	120.330	5.0	6.1
7	花東縱谷地震系列	1951/10/22 05:34	23.875	121.725	4.0	7.3
		1951/10/22 11:29	24.075	121.725	1.0	7.1
		1951/10/22 13:43	23.825	121.950	18.0	7.1
		1951/11/25 02:47	23.100	121.225	16.0	6.1
		1951/11/25 02:50	23.275	121.350	36.0	7.3
8	恆春地震	1959/08/15 16:57	21.700	121.300	20.0	7.1
9	白河地震	1964/01/18 20:04	23.200	120.600	18.0	6.3
10	花蓮地震	1986/11/15 05:20	23.992	121.833	15.0	6.8

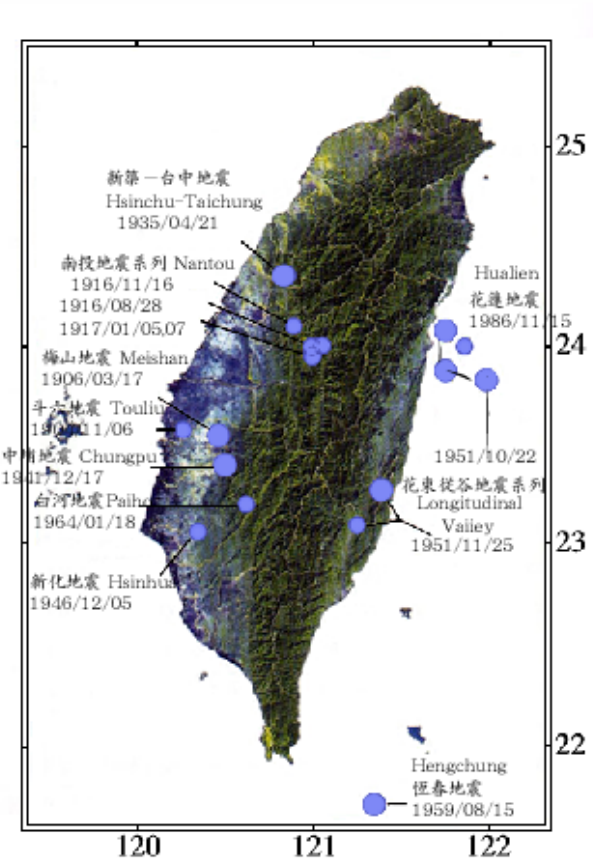

Figure 3.2 Large historical events in of Taiwan
http://www.sinica.edu.tw/~jclee/921chichi_10big.htm

Figure 3.3 The contour map of the number of earthquakes occurred in 1904

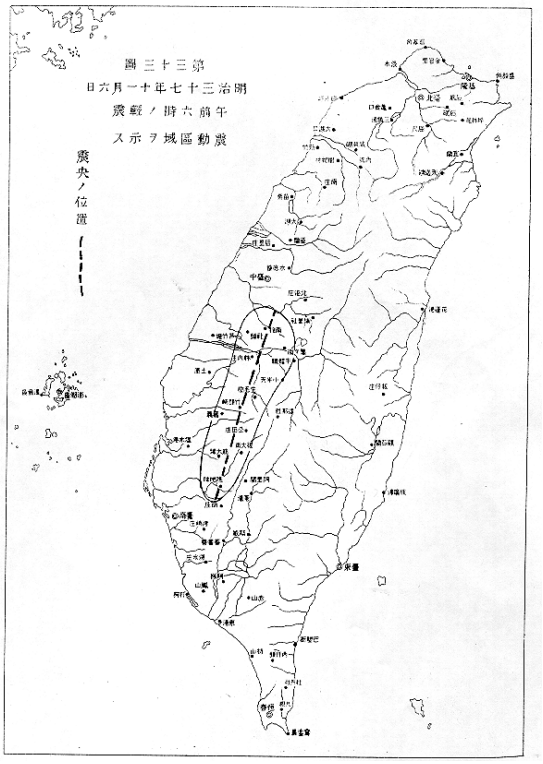

Figure 3.4 The strongly affected area

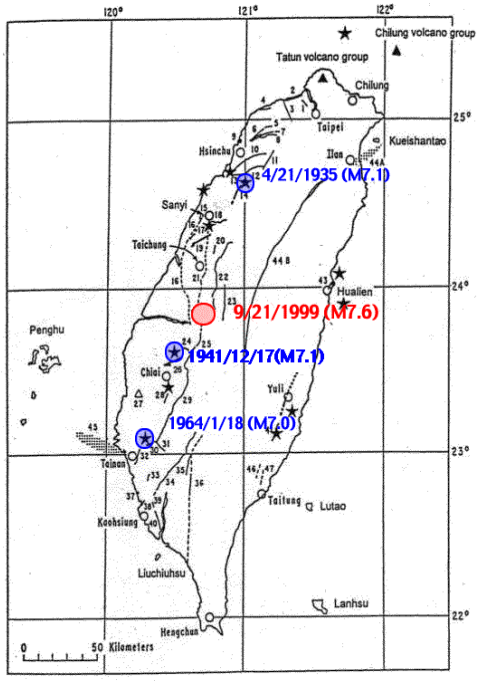

Figure 3.5 Destructive earthquakes occur along the Western Foothills from Chutung to Tainan (Bonilla,1977)
http://www2.rcep.dpri.kyotou.ac.jp/~sato/taiwan/recent.html

REFERENCE

Ohmori, F. (1906), Taiwan Earthquake Report, *The Contents of Publications of the Imperial Earthquake Investigate Committee*, No.54. pp.104-123.

Bonilla, M.G.(1977), Summary of Quaternary faulting and elevation changes in Taiwan, *Geol. Soc. China,* Mem. 2, pp.43-55.

3.3 Main Shock and Aftershocks

At 1:47 a.m. local time on Tuesday September 21 (17:47 GMT on Monday September 20), 1999, a main shock with magnitude 7.3(CWB) occurred in Ji-Ji, Nantou County. The epicenter of the earthquake was at 23.85 degrees latitude and 120.81 degrees longitude. The depth of hypocenter was about 6.99 km. The surface ruptures appeared in a NS direction along the foothill over 80 km in length. Source mechanism by CMT Solution of Earthquake Research Institute (Univ. of Tokyo) indicates a reverse dip-slip fault as shown in Figure 3.6.

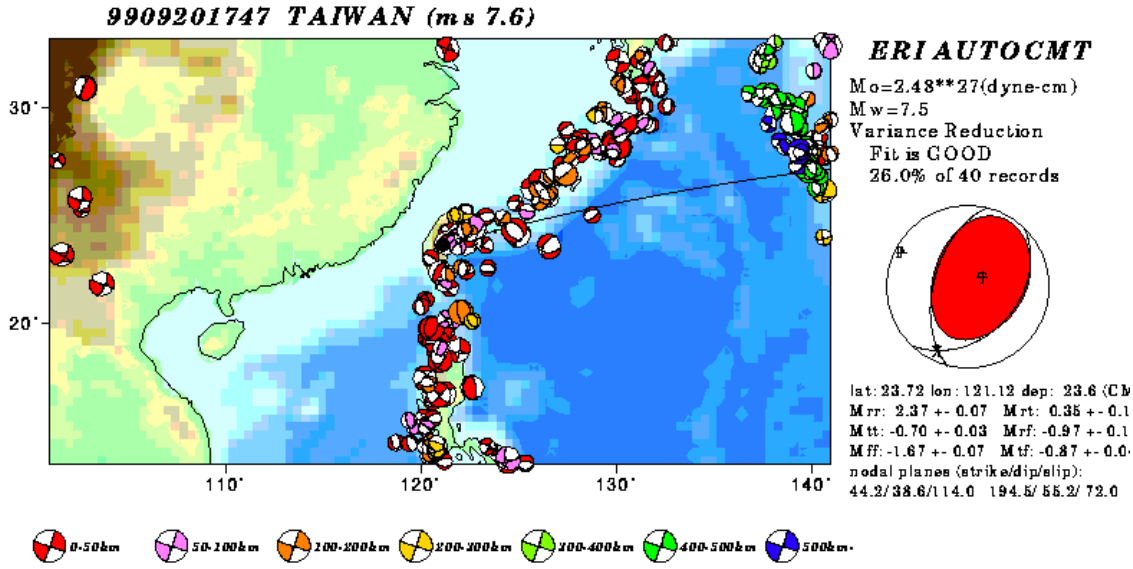

Figure 3.6 CMT Solution determined by Earthquake Research Institute (Univ. of Tokyo)

http://www.eri.u-tokyo.ac.jp/~http/CMT/9909201747.gif

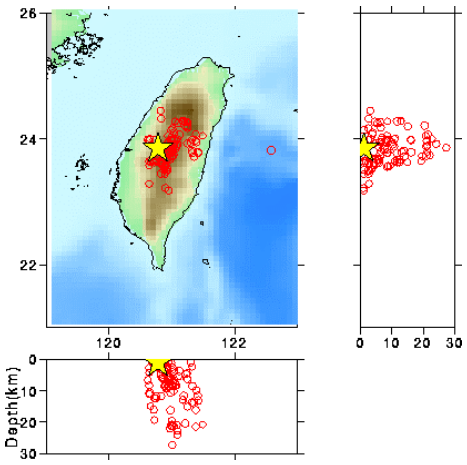

According to the Central Weather Bureau of Taiwan, the depth of hypocenter of main shock was shallow as shown in Figure 3.7. Based on the after shock distribution the fault rupture propagates from the shallow part of the fault plane to deep part and spread to both north and south directions. Figure 3.8 shows the hypocenter of main shock and distribution of aftershocks occurred up to 26 September, 1999.

Figure 3.7 The distribution of aftershocks (determined by Central Weather Bureau)

http://wwweic.eri.utokyo.ac.jp/topics/taiwan/yoshin2e.html

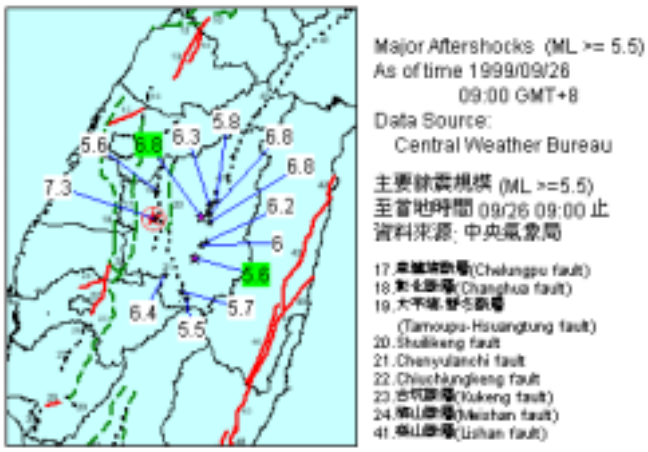

Figure 3.8 The distribution of aftershocks (determined by Central Weather Bureau)

The source mechanism determined by Yagi and Kikuchi was a reverse fault with a strike of NNE-SSW. Their result revealed that a small introductory rupture with a duration of 10 sec was followed by a few bigger subevents. The rupture front velocity is about 2.5 km/sec. The rupture eventually swept over the length of 50 km to NE and 30 km to SW and the width of about 40 km (see Figure 3.9). The area of maximum stress drop occurred is not coincide with the hypocenter area but located lather north east region.

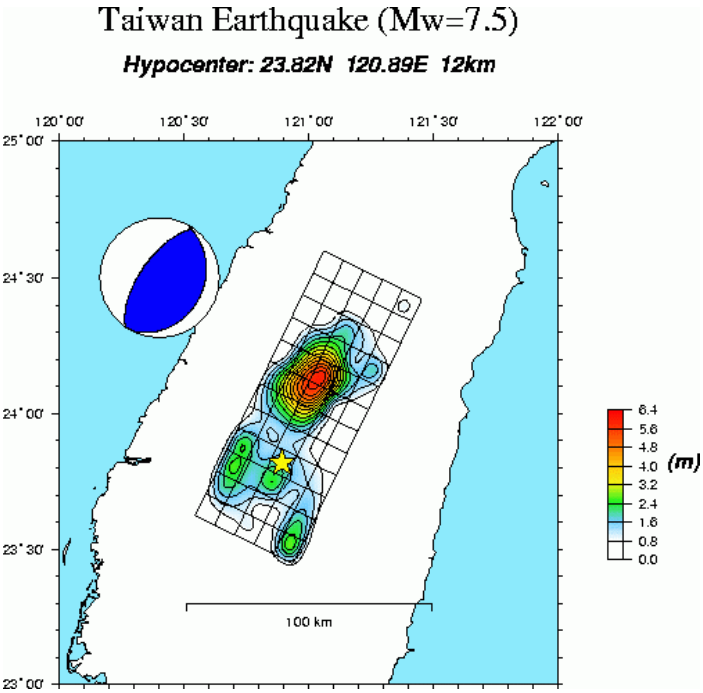

Epicenter = 23.82N, 120.89E

(strike, dip, slip) = (26, 27, 82)

(HRV CMT)

Seismic moment

Mo = 2.4 x10**20 Nm

(Mw = 7.5)

Source duration T = 28 s

Centroid depth H = 11 km

Rupture area S = 80 km x 40 km

Averaged dislocation D = 2.2m

Averaged stress drop = 3.3 MPa

Figure 3.9 Distribution of fault-slip determined by the result by Yagi & Kikuchi (1999).

http://wwweic.eri.u-tokyo.ac.jp/yuji/tai/tai.html

3.4 Geology and Ground Characteristics

3.4.1 General Geology in Western Taiwan

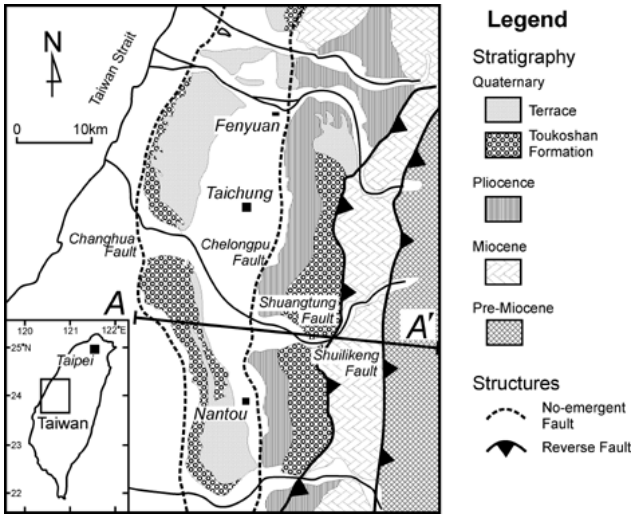

Figure 3.10 Schematic map of the fault traces and general geology of the 1999 Ji-Ji earthquake region (modified after Ho, 1986) http://caldera.wr.usgs.gov/chi-chi4.html

The Chelungpu and Shuangtung faults, which caused this earthquake, is a typical active fault of Western Taiwan. These faults are 10 km apart and sub-parallel in the western foothills. Figure3.10 is a schematic map of the fault traces and general geology of the Ji-Ji earthquake region.

According to Central Geological Survey report (Ho, *et al*., 1988), geologic province of the western foothills is the site of a Late Cenozoic sedimentary basin west of the Central Range. Major orogeny began in early Pleistocene time, and all the sedimentary units in this western basin have been folded and faulted to form the geologic structures of the western foothills (see Figure3.11).

A gradual change in Miocense stratigraphy from northern Taiwan toward central and southern Taiwan is reflected in lithologic character. The thickness of Moicene units seems to increase gradually toward the south. Pliocene units are distributes in the hills and lowlands west of the exposed Miocene strata in the western foothills.

The Tertiary strata of the western foothills have been flexed into folds that trend E-NE to N-NE, each one to several km across. Most folds are asymmetric and have been pushed over toward the NW by a strong force coming from the E or SE. With increase of the NW push, the strata on the steep limbs have commonly been broken through by W-verging thrust fault (see Figure3.12). Most of thrusts are with very low dip angle and bedded over certain distances.

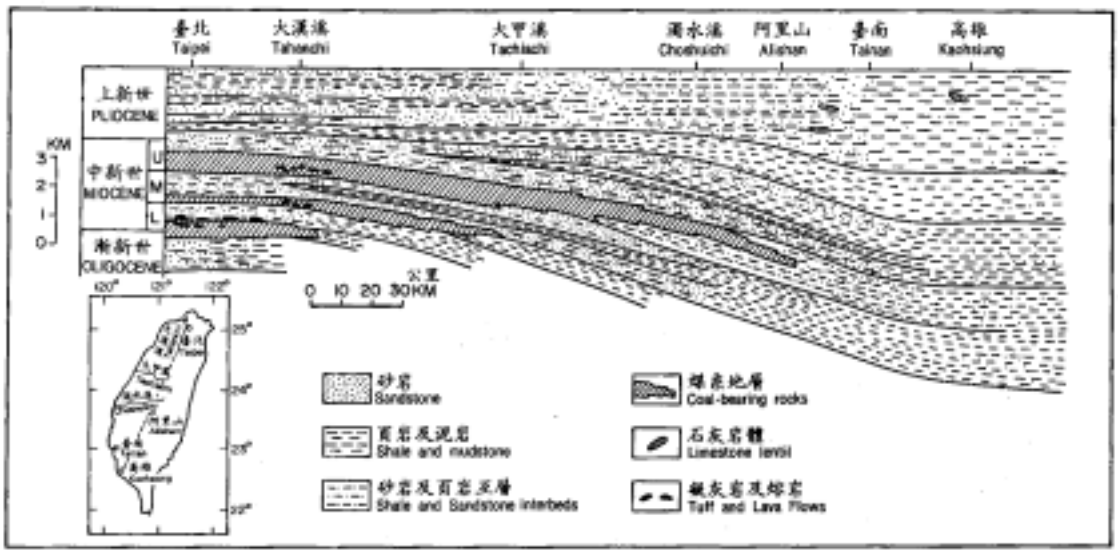

Figure 3.11 North-south facies change in the sedimentary basin of the western foothills, showing variation of lithology and thickness of Neogene rocks (after Ho,*et al.*, 1988).

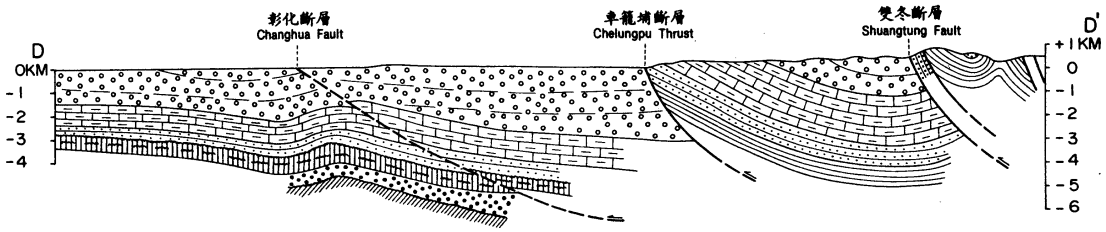

Figure 3.12 Structure cross sections of western foothills (after Ho,*et al.*, 1988)

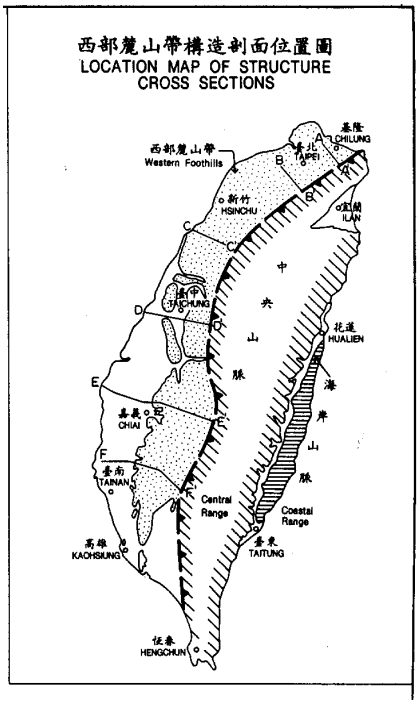

REFERENCE

C.S.Ho(1988), An Introduction to the Geology of Taiwan Explanatory Text of the Geologic Map of Taiwan, Central Geological Survey report .

3.4.2 Estimates of ground-motion characteristics in Wu-Fong

Figure 3.13 shows a local map including Taichung and the epicentral region. The level of peak ground acceleration (PGA) at a strong motion observation station is indicated by a diameter of circle in the figure. PGA decreases as the epicentral distance increases and most of PGAs around Taichung are smaller than 0.4g. Ground motions on the hanging wall are usually stronger than those on footwall. This means that the ground motion is strongly affected by the fault mechanism. However, a few stations on the footwall recorded high PGAs. For example, PGA at Wu-Fong are quite higher than Chaotuen although both strong-motion stations are located on the footwall. Figures 3.14 and 3.15 show time histories of observed earthquake motions at Wu-Fong and Chaotuen, respectively. Note that each scale is normalized to the maximum amplitude. The peak ground accelerations are 0.79g at Wu-Fong and 0.33 at Chaotuen. The predominant period of the Wu-Fong record seems to be longer than that of Chaotuen. There is a possibility that the ground motion was amplified due to local site effects.

To obtain ground amplification characteristics in Wu-Fong, microtremor observations were carried out in the city. Observations were made from 5:30am to 8:00am on October 5, 1999. Figure 3.16 shows an example of microtremors observed at a site (Wu-Fong02) where two building had been totally collapsed due to differential settlementrs (see Figure 3.17). Figure 3.18 shows an example of microtremors observed at a site (Wu-Fong06) where the soils around apartment buildings had subsided and pavement fissures occurred along the buildings due to the subsidence (see Figure 3.19). No sand boils were observed at the land-settlement sites.

Figure 3.4.20 shows the spectral ratios of horizontal-to-vertical components of microtremors (H/V spectral ratios) using the technique proposed by Nakamura (1989). To obtain the spectral ratios, three sets of 20.48-sec-long records sampled at 100 Hz were selected. Fourier spectra of the records were calculated and then smoothed with a 0.5-Hz Parzen window. The horizontal spectra were divided by the vertical spectra, then the ratios were arithemetically averaged.

It is found that the H/V spectral ratios at both sites have marked spectral peaks; 0.8 sec at Wu-Fong02 and 0.9 sec at Wu-Fong06. Some native people told that the city is underlaid by silty or clayey deposits and some part of the city had been originally fish

ponds. The strong-motion records, microtremor records, and the comments of the native people suggest that the city has thick and soft subsurface soils which might cause the land settlements and ground-motion amplification during the earthquake.

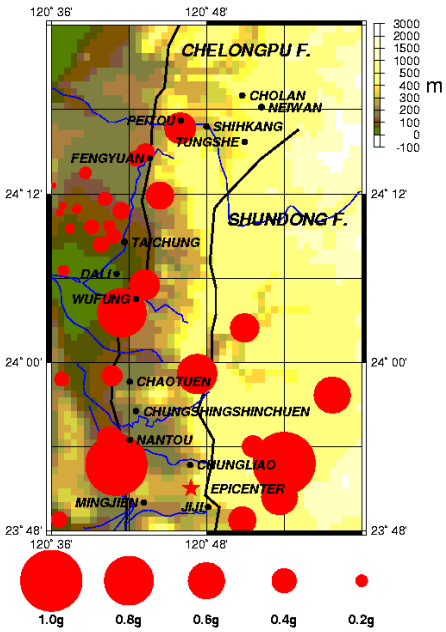

Map of the epicentral region and observed PGA

Figure 3.13 Map of the epicentral region and observed PGA.

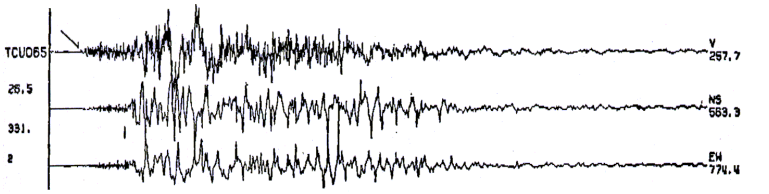

Figure 3.14 Main shock time histories observed in Wu-Fong (TCU065: Wu-Fong elementary school) .

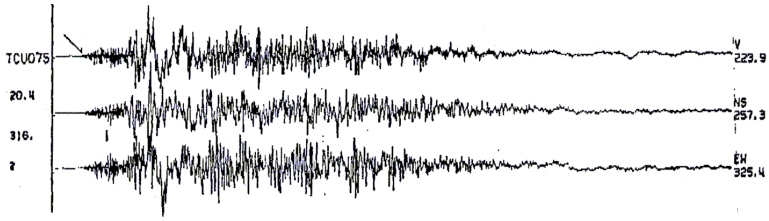

Figure 3.15 Main shock time histories observed in Chaotuen (TCU075: Chaotuen elementary school).

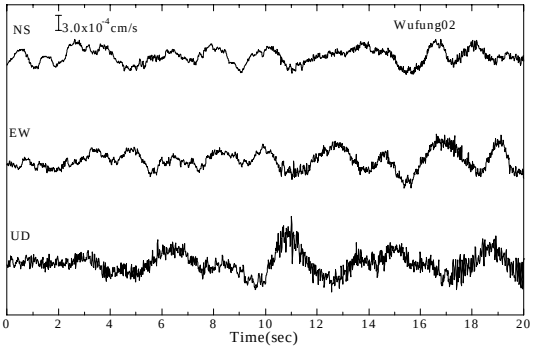

Figure 3.16 Microtremor records observed in Wu-Fong (Wufung02).

Figure 3.17 Microtremor observation in Wufung (Wufung02).

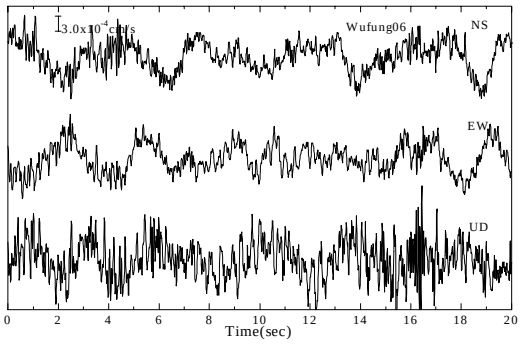

Figure 3.18 Microtremor records observed in Wu-Fong (Wufung06).

Figure 3.19 Microtremor observation in Wu-Fong(Wufung06).

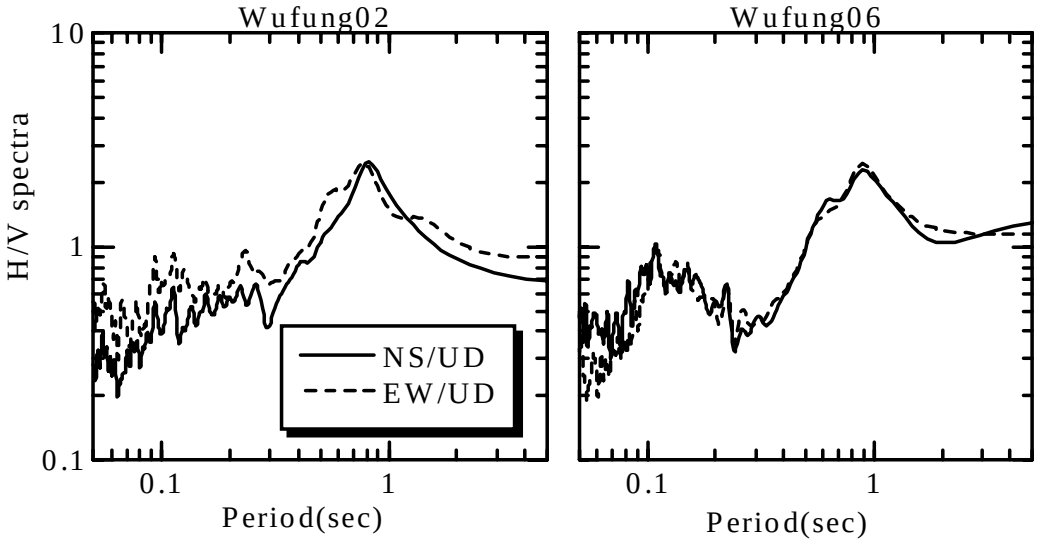

Figure 3.20 H/V spectral ratios at damaged sites in Wu-Fong (Wufung02 and Wufung06).

REFERENCE

Nakamura, Y. (1989). A method for dynamic characteristics estimation of subsurface using microtremor on the ground surface, QR. Of RTRI, 30, No.1, 25-33.

3.5 Surface Fault Trace

Static displacements at observation stations obtained by integrating recorded accelerations along the Chelungpu fault are shown in 3.21. Both vertical and horizontal displacements at northern stations are larger than those of southern part. More than 7 m vertical displacement at the Shi-Kan observation station can be seen. The EW component of static displacement is lager than the NS component. The static displacement of hanging wall side is lager than that of footwall. These are coherent with surveyed surface dislocations of Chelungpu fault and the distribution of fault-slip vector determined by Yagi and Kikuch (Figure 3.9).

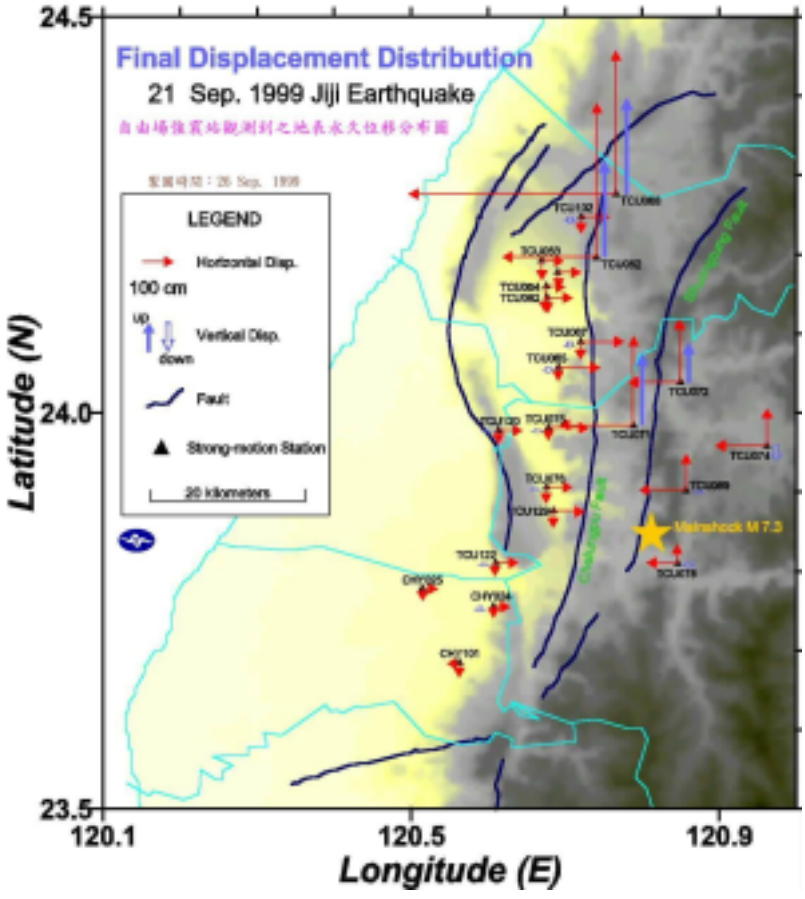

Figure 3.21 The final displacement distribution

http://www.cwb.gov.tw/Data/earthquake/921moving.jpg

3.5.1 Miauti sheu Nei-Wan

At Nei-Wan, which is located in the North-end part of the Chelungpu fault, a distinct fault was found, showing 5 m displacement in the vertical direction (Photo 3.1). Furthermore, surface ruptures extended to North-East direction. This photograph is

taken from the east. Photo 3.2 was an agricultural road deformed by the surface displacement located at about 50 m left of the location shown in Photo 3.1, and this photograph was taken from the south. Photo 3.3 was taken from the south at the point where Photo 3.2 was taken, and the surface ruptures can be seen in the east-west direction expressing by extended arms in the photograph. Appearance of surface ruptures was complicated in the north-end part of the fault and the surface ground movement caused by the dislocation of deeper part of the fault could not be simply explained by upward deformation of hanging wall. This kind of complexity usually can be seen for the case of a back-thrust fault. If a back-thrust occurred in a thrust belt an upheaval hinterland called pop-up phenomenon can be seen as illustrated by Figure 3.22.

S←　　→N

Photo 3.1 Road deformation in Nei-Wun①

W←　　→E

Photo 3.2 Agricultural road deformation ②

W←　　→E

Photo 3.3　Surface ruptures(East and West) ③

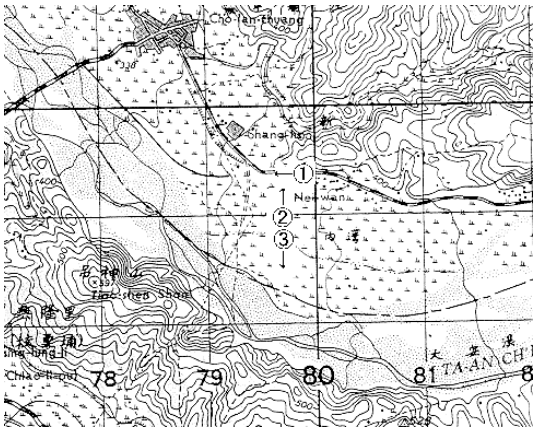

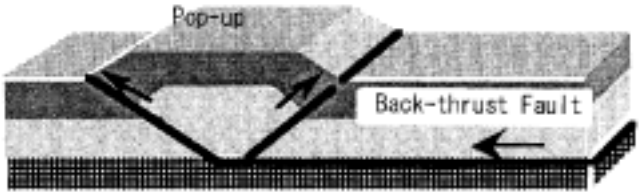

Figure 3.22 Back-thrust fault and pop-up

3.5.2 Circumference of Shih-Yuen Bridge

This place is northern part of the Chelungpu fault. The fault with a strike of NE-SW was running across under Shih-Yuen Bridge. Most of damage to the bridge was induced by the fault (Photo3.4).

A landslide occurred near the left bank of Shih-Yuen Bridge. The house in Photo 3.5 moved about 8 m from the original position to the right-hand side of the photograph according to the landslide. Due to the ground movement the structural foundation distorted. Large surface rupture was also appeared at a surrounding of ground surface (Photo3.6).

Photo 3.4 Collapsed bridge of Shih-Yuen Bridge located in the northeast of the Shikan Dam

Photo 3.5 Movement of the house by the landslide

Photo 3.6 The surface rupture was appeared in near

3.5.3 At Shye-Gang Dam and Pei-Fong Bridge

The fault crossed the edge of Shye-Gang Dam. A large vertical displacement created by the fault movement. According to a leveling conducted by the dam control organization the floodgate side uplifted 9.8 m and right-bank uplifted about 2 m (Photo3.8-3.9). The road which ran along the right bank side of the dam to a downstream, there was about 5 m deformation in the vertical direction. Pei-Fong Bridge is a bridge located lower streamside of Shye-Gang Bam.

Tow beams were corrupted. The waterfall appeared at the NE-SW direction, showing about 2 and 3 m uplift of upper streamside (Photo 3.9). The surface rupture by the fault goes up north in the right-bank side.

Photo 3.7 Uplift of floodgate (9.8 m) and right-bank abatement (2 m)

Photo 3.8 A photograph of damaged situation dam taken from the lower stream of a river (by Konagai)

Photo 3.9 The waterfall appeared at the NE-SW direction

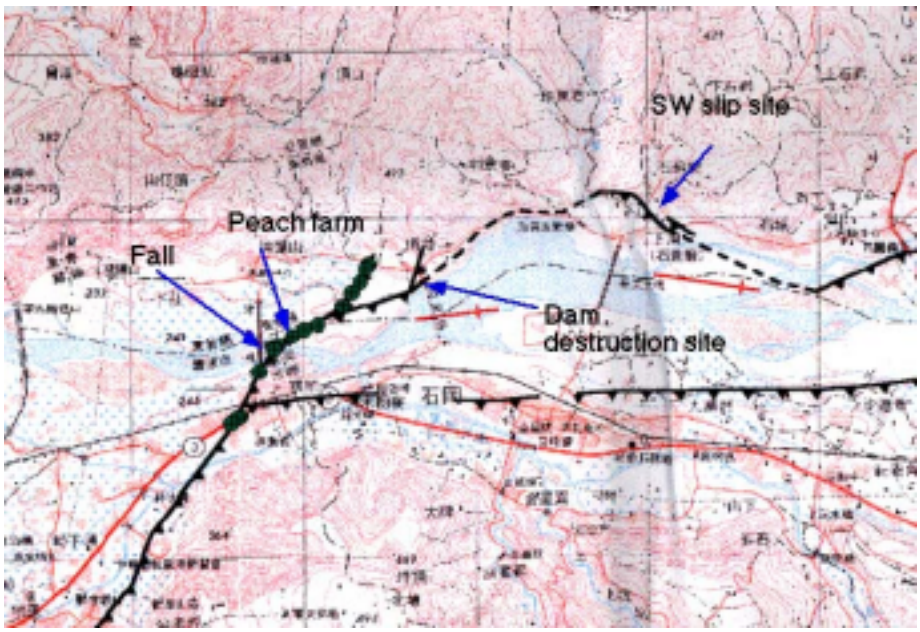

Figure 3.23 Traces of surface ruptures surveyed by Central Geol Survey (modified after Seno)
http://www.eri.u-tokyo.ac.jp/seno/analogue.eng.html

3.5.4 Fong-Yuan Tuu-Nyu Tsuen

In Fong-Yuan area, the surface rupture can be seen at the east side of Route 3 which runs parallel to the fault traces from the north to south. Damage to structures caused by surface ruptures due to the fault movement was very severe but restricted in a small area within the distance of several tens meters from a surface rupture (Photo3.10-11).

Photo 3.10 Route 3 at Tuu-Nyu Tsuen.

Photo 3.11 Damage to structures caused by surface ruptures

3.5.5 Jiungung elementary school, Wu-Fong Shiang athletics ground

Jiungung elementary school and Wu-Fong athletics ground are located in the middle of the Chelungpu fault. At Jiungung elementary school, the surface rupture was appeared on the pavement ground (photo3.12). At Wu-Fong Shiang athletics ground, a distinct surface trace of the fault movement with about 2 m vertical displacement could be seen on the all weather (en-tout-car) track (Photo3.13). The vertical displacement was predominated even though a small horizontal displacement is recognized(Photo3.14).

Photo3.12 The appeared fault with NS strike on the pavement ground

Photo3.13 Wu-Fong Shiang athletics ground

Photo3.14 A small horizontal displacement is recognized

REFERENCES

Kano, K., Murata, A.(1998), Structural Geology (Kouzou Chishitsu Gaku in Japanese) , Asakura Publishing Co.,Ltd., ISBN4-254-16237-5.

3.6 Observed Record

The Central Weather Bureau (CWB), Ministry of Transportation and Communications, Taiwan is operating a rapid earthquake information release system (Figure 3.24). The main shock motions were recorded at more than 500 observation stations. The maximum accelerations at the TCU129 observation station (13.2 km west of the epicenter at Ji-Ji) were 983.0 gal (EW component), 610.7 gal (NS component) and 335.0 gal (UD component). The time histories of accelerations records (UD, NS, and EW components) are shown in Figure 3.25 at the observation stations CHY006 (Mei-Shan elementary school, epicentral distance of 65.4 km) and CHY024 (Lin-Jong elementary school, epicentral distance of 23.1 km) which are located southern side of the epicenter, TCU129 (Sin-Wei elementary school), as well as TCU052 (Gwang-Jeng elementary school, epicentral distance of 39.2 km) and TCU068 (Shen-Gang elementary school, epicentral distance of 47.6 km) which are located northern side of the epicenter. Near the epicentral region the acceleration time history contains high frequency components and has long duration. On southern side of epicenter the tendency to predominate high frequency still exists although the duration becomes shorter as the epicentral distance increases. However on the northern side of the epicenter the predominant period becomes longer as the epicentral distance increases. The predominated period range is 1-3 seconds (see Figure 3.25) and a pulse like wave form can be seen at the observation site TCU068. These characteristics of observed records are dependent on the rapture mechanisms of earthquake fault. Due to the complicated tectonic environment of Tawian the rupture mechanism may not be so simple. But fortunately based on CWB efforts earthquake motions of the main shock were recorded by the densely distributed stations in the near source region. Using observed strong ground motions the source mechanism will be studied in detail by seismologists in the future. Studies to make clear the relationship between damage to structures and ground motions will also be conducted. Lack of observation stations in mountain region will, however, be disadvantage to analyze severe slope failures occurred in the mountain area.

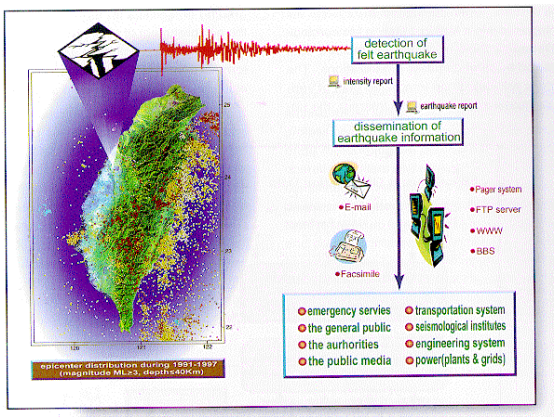

Figure 3.24 The Taiwan Rapid Earthquake Information Release System(TREIRS)

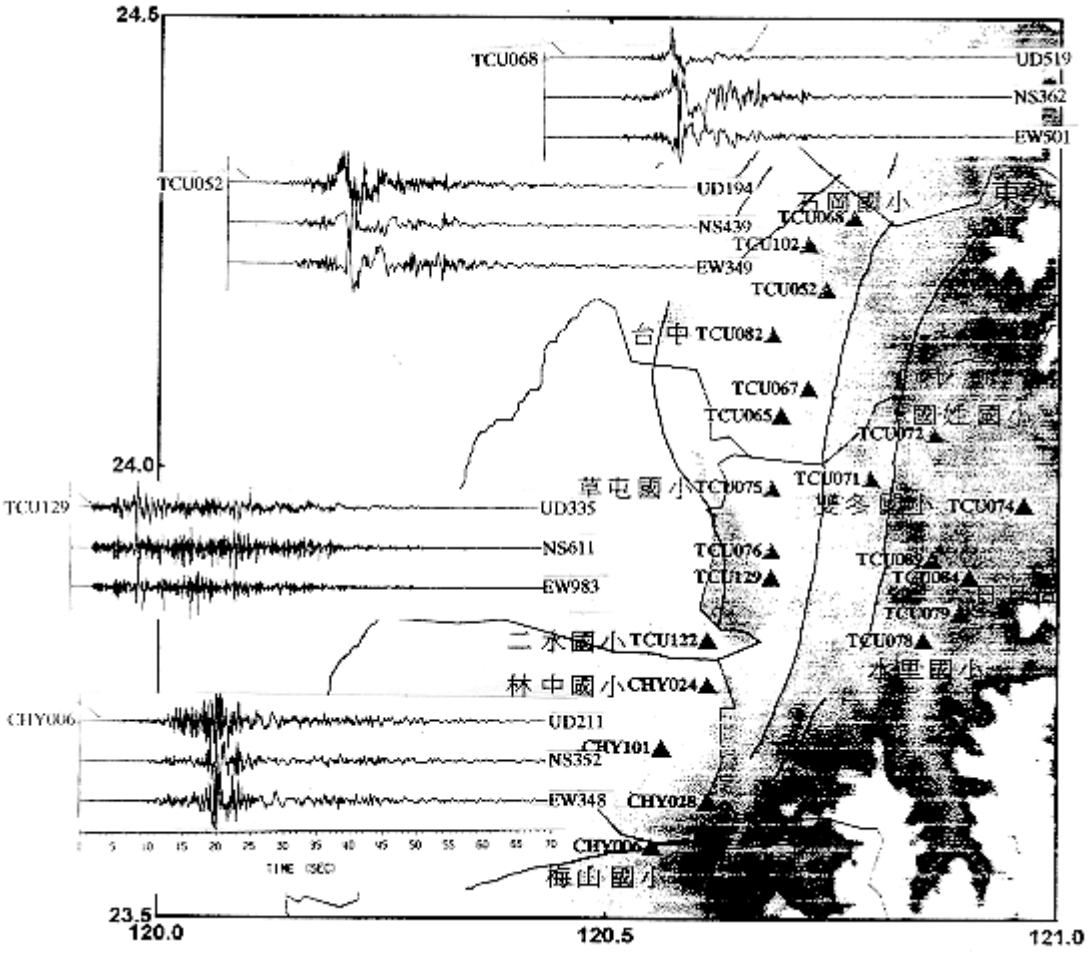

Figure 3.25 The CWB recorded ground motions(TCU068,TCU052,TCU129,CHY006)

Figure 3.26 shows the contour lines of peak acceleration of NS and EW components. The maximum value of contour in NS component is 700 gal and its shape is long and narrow in north-south direction. A small island of contour with 600 gal can be seen at the north end of earthquake fault. The maximum vale of contour of EW component is 800 gal and its configuration is a little bit thick in east-west direction. One of reasons that maximum accelerations of EW component are lager than those of NS component is simply explained by the radiation pattern of the S wave.

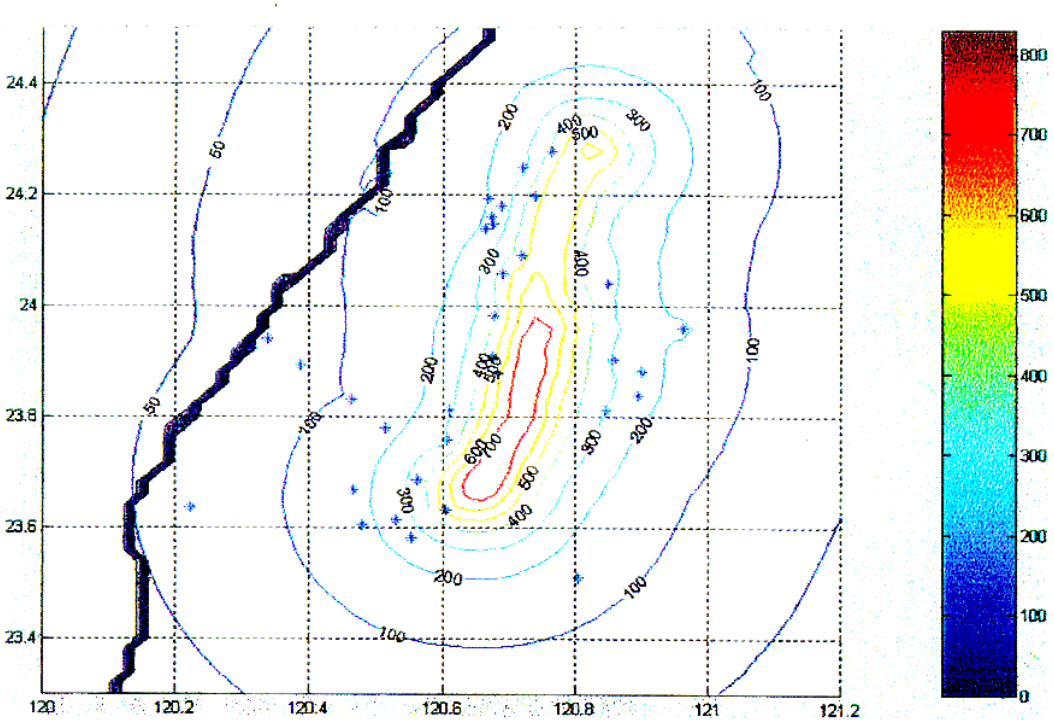

Figure 3.26*a* PGA-NS component distribution(Provided by Prof.Loh)

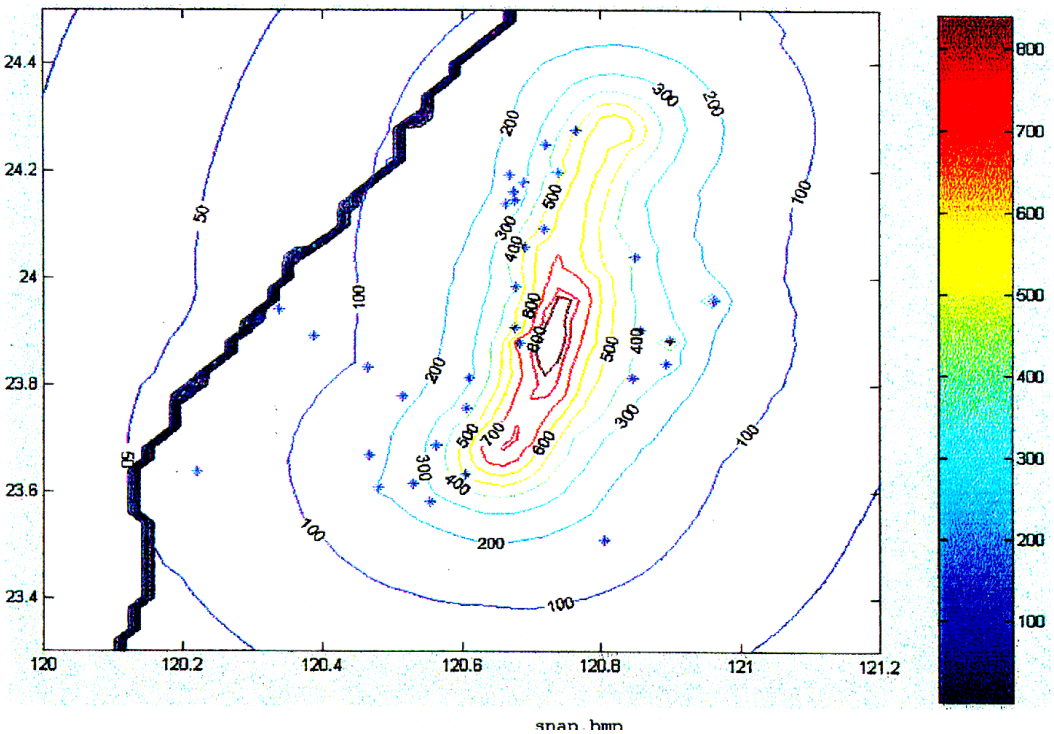

Figure 3.26*b* PGA-EW component distribution(Provided by Prof.Loh)

Figures 3.27 and 3.28 show acceleration spectra calculated using observed records near the source region. From spectra shown at lower left hand side of Figure 3.27 we can see that longer period motion predominates as the distance from the Chelungpu fault increases but this tendency reverses as observation sites approaches to the seaside. This means that there is a deep valley like hard irregular ground profile between the east side mountain range and the west side seashore. The lower right hand side spectra are from the records observed at stations located near the south end of the Chelungpu fault. Not so much difference can be seen. Spectra at the observation stations located at east side of the Chelungpu fault show that the longer period predominates as going up from south to north along the fault.

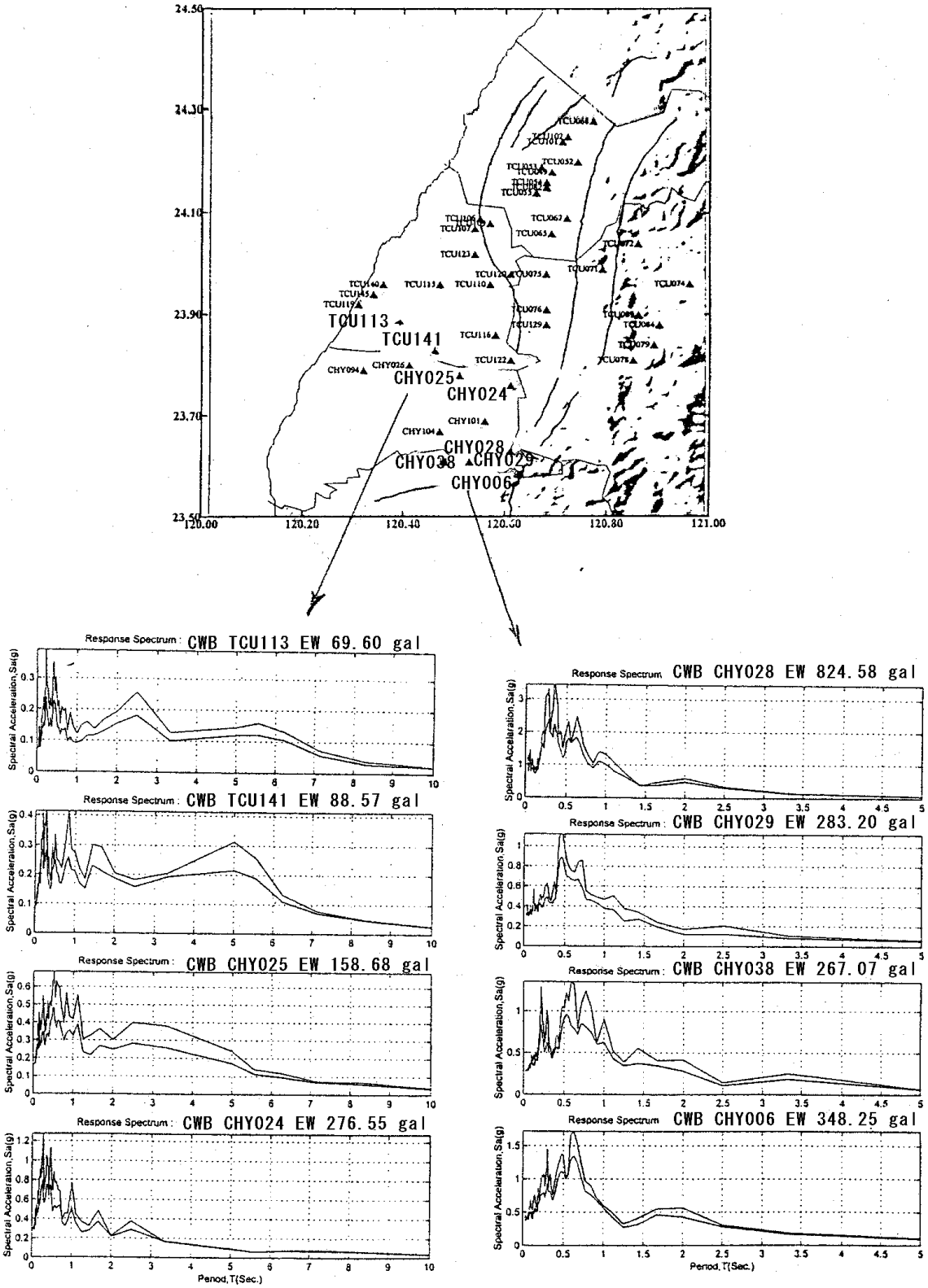

Figure 3.27 Comparison of record observed on the western side from the dislocation

(Provided by Prof.Loh)

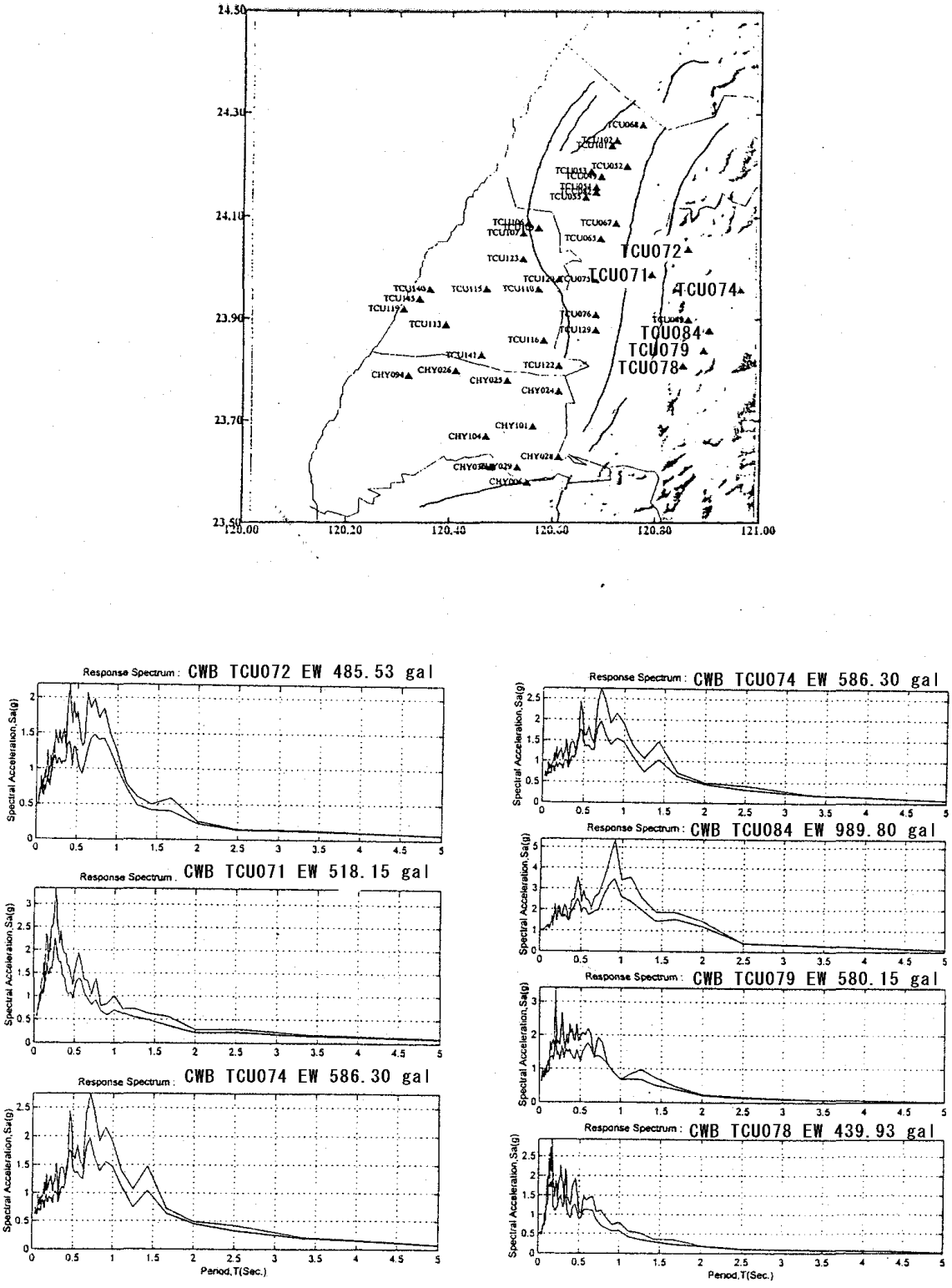

Figure 3.28 Comparison of record observed on the eastern side from the dislocation

(Provided by Prof.Loh)

3.7 Characteristics of seismic record observed at Taichung city

In many seismic motions recorded during The 1999 Ji-Ji earthquake we here investigate characteristics of an earthquake ground motion recorded on the ground surface in the campus of National Chung-Hsing University. The seismograph has been installed and maintained by Dr. Chi-Chang Lin, Professor from Department of Civil Engineering. The university is located in the southern part of Taichung city. According to the soil condition at the observation site, the soil profile and the distribution of shear wave velocity with depth are shown in Figure 3.29 The soil layer below the depth of GL-2 m consists of sandy gravel. The water table is at about GL-2.7 m.

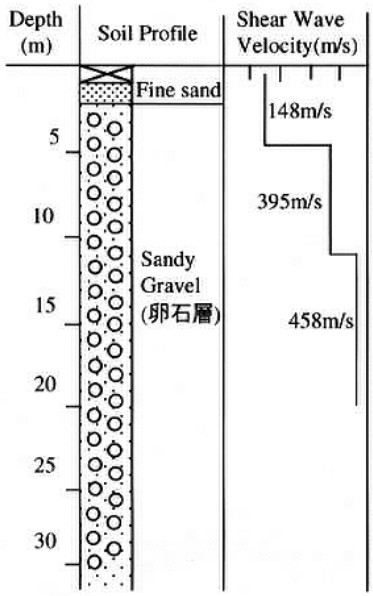

Figure.3.29 Soil Profile at Seismic Observation site In National Chung-Hisng University

The shear wave velocity below the depth of GL-5 m is beyond 395 m/sec. These data were provided by Dr. Ding-Lien Lin, Professor of Department of Civil Engineering, National Chung-Hsing University.

Acceleration time histories of three components are shown in Figure 3.32. The maximum acceleration of EW component is larger than that of NS component. The maximum acceleration of vertical component is almost half of the EW component. The amplitude characteristic of EW component changes drastically at about 10 seconds after arrival of S wave. To make clear this evidence the non-stationary spectrum of vertical component time history is shown in Figure 3.31. The strong non-stational characteristic beyond a period of 2.0 second is remarkable in the spectrum, especially the later part of time history of recorded motion.

Acceleration and velocity response spectra (h=5%) are shown in Figure 3.32. For the comparison those calculated from the records at GL-83m of Port Island observed during the 1995 Hyogoken-Nanbu earthquake. These response spectra were calculated by a composed time history of two horizontal components. The maximum acceleration amplitude of the 1995 Hyogoken-Nanbu earthquake is almost twice to that of the Ji-Ji earthquake. However, response spectrum of the Ji-Ji earthquake at periods beyond 2.0

second is larger than that of the 1995 Hyogoken-Nanbu earthquake. Especially, the velocity response at the period beyond 2.0 second exceeds 100m/s. This evidence is one of peculiar characteristics of the Ji-Ji earthquake ground motion.

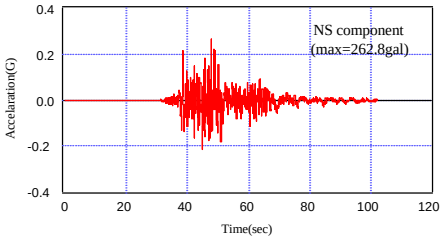

a)NS Component

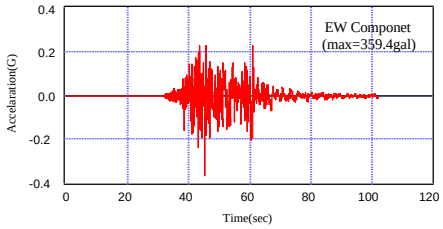

b)EW Component

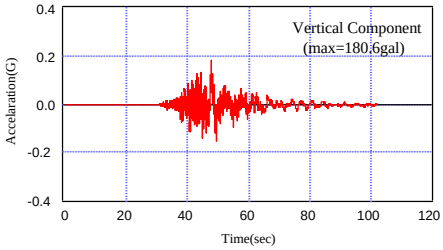

c)Vertical Component

Figure 3.30 Acceleration Time histories

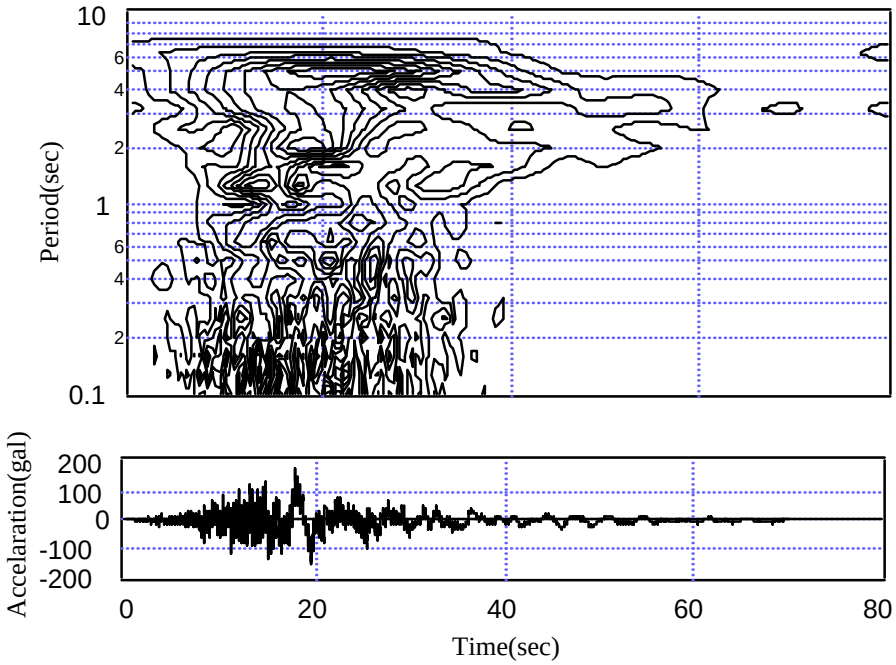

Figure 3.31 Non-Stationary Spectrum of Vertical Component

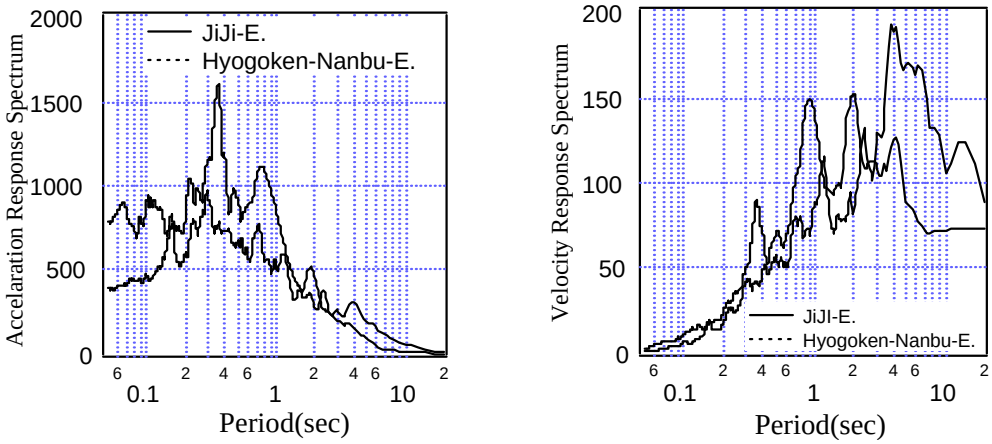

a) Acceleration Response Spectra b) Velocity Response Spectra

Figure 3.32 Comparison of Response Spectra (h=5%) between the 1999 Ji-Ji and 1995 Hyogoken-Nanbu earthquakes

As an example of damage to structures caused by such low frequency component of the earthquake motion, the failure of a cone-type roof slab of the molasses tank at Taichung port is shown in Photo 3.15.

The cross section of the tank is shown in Figure 3.33. The natural period and maximum liquid surface displacement caused by the sloshing of molasses in the tank were calculated by using Houser's velocity potential theory. The height of molasses before the earthquake assumed to be 10.5m based on the information about the amount of the molasses being about 90% of filled condition. The calculated natural period is 5.2 second and the maximum liquid displacement is more than 1.6 m. The velocity spectrum value at this period is assumed to be from 170m/s to 100m/s even taking into account an attenuation effect between Taichung city and Taichung Port. The failure of the ceiling slab of the tank seems to be caused by the sloshing of molasses due to the very high velocity spectrum amplitude at such a longer period.

Photo 3.15 Damage of the Molasses Tank
(Provide by The investigation team for The 1999 Ji-Ji Earthquake by The Japanese Geotechnical Society)

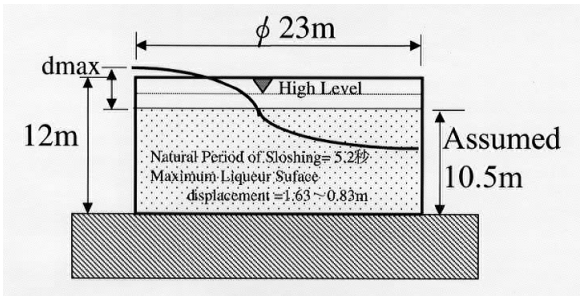

Figure 3.33 Cross Section of the Molasses Tank

3.8 Conclusion

The 1999 Ji-Ji earthquake was a thrust type earthquake and about a 80 km trace of surface fault was appeared. Damage to infrastructures caused by the fault dislocation was very severe but it concentrated near the surface trace of the fault. The hanging wall of this earthquake fault was on the mountainside. Damage could be much worse if the densely populated area was located on the hanging wall. What we have learned form the 1995 Hyogoken Nanbu earthquake was only the damage caused by a strike slip type fault and with no surface trace in the densely populated area. There are several active faults in Japan of which source mechanisms are similar to the Ji-Ji earthquake. We can learn many aspects of on this earthquake and reflect learned knowledge to prevent damage from future earthquakes in Japan.

In 1999 there were many earthquakes such as Kocaeli (Turkey) earthquake (*Mw* 7.4; 17, Aug.), Athens (Greece) earthquake (*Mw*5.9; 7, Sep.), Oaxaca (Mexico) earthquake (*Mw*7.3; 30, Sep.), Hector Mine (U.S.A.) earthquake (*Ms* 7.3; 16, Oct.). The earth seems like to enter to an earthquake prone period. Without exception we have to face to a new type of earthquake damage in the near future. Oure duty is to develop preventive measures to future earthquakes based on the knowledge learned from these earthquakes.

The research level of earthquake engineering in Taiwan is one of the highest in the world. We have a long history of exchanging science and technologies with Taiwan. During we stayed in Taiwan to survey this earthquake damage we had very friendly supports from Taiwan side. What kind of official supports for restoration process we can offer from Japanese side as the member of Japan Society of Civil Engineers is an important issue.

Acknowledgements

We would like to express our gratitude to many researchers in Taiwan who took care of us during our reconnaissance, October 1 - 12, 1999, especially Professor Chin-Hsiung Loh form National Taiwan University and director of the National Center for Research on Earthquake Engineering to instruct us global information of the Ji-Ji earthquake and to issue official permission passes to enter the damaged area as well as Professors Chi-Chang Lin and Ping-Lien Lin from National Chung-Hsing University to instruct us the damage in Taizhong area, and to provided us the seismic record as well as the information of the soil profile about their seismic observation.

We also thank to many web sites which we have referred to write this report, especially Central Weather Bureau in Taiwan, Earthquake Research Institute of the University of Tokyo and Disaster Prevention Research Institute of Kyoto University.